Kidney360

Mannose Binding Lectin Is Hydroxylated by Collagen Prolyl-4-hydroxylase and Inhibited by Some PHD Inhibitors

Vijesh J. Bhute[1], *James Harte*[2,3], *Jack W. Houghton*[1] and *Patrick H. Maxwell*[1]

Abstract

Background Mannose-binding lectin (MBL) is an important component of innate immune defense. MBL undergoes oligomerization to generate high mol weight (HMW) forms which act as pattern recognition molecules to detect and opsonize various microorganisms. Several post-translational modifications including prolyl hydroxylation are known to affect the oligomerization of MBL. Yet, the enzyme(s) which hydroxylate proline in the collagen-like domain residues have not been identified and the significance of prolyl hydroxylation is incompletely understood.

Methods To investigate post-translational modifications of MBL, we stably expressed Myc-DDK tagged MBL in HEK293S cells. We used pharmacologic and genetic inhibition of 2-oxoglutarate–dependent dioxygenases (2OGDD) to identify the enzyme required for prolyl hydroxylation of MBL. We performed mass spectrometry to determine the effects of various inhibitors on MBL modifications.

Results Secretion of HMW MBL was impaired by inhibitors of the superfamily of 2OGDD, and was dependent on prolyl-4-hydroxylase subunit α1. Roxadustat and vadadustat, but not molidustat, led to significant suppression of hydroxylation and secretion of HMW forms of MBL.

Conclusions These data suggest that prolyl hydroxylation in the collagen-like domain of MBL is mediated by collagen prolyl-4-hydroxylase. Reduced MBL activity is likely to be an off-target effect of some, but not all, prolyl hydroxylase domain (PHD) inhibitors. There may be advantages in selective PHD inhibitors that would not interfere with MBL production.

KIDNEY360 1: 447–457, 2020. doi: https://doi.org/10.34067/KID.0000092020

Introduction

Each mannose-binding lectin (MBL) peptide consists of a tail with a collagen-like domain and a calcium-dependent carbohydrate recognition head which can detect mannose and other carbohydrates in microbial cell membranes (1,2). In addition to binding to pathogens, MBL has also been reported to bind to apoptotic cells (3). Mice lacking MBL (4) are reported to be protected against cardiac reperfusion injury, supporting a role for MBL in the inflammatory response. A recent study also reported experimental evidence for a role of MBL in accelerating pancreatic ductal adenocarcinoma in mice by activating the complement pathway in response to *Malassezia* species of fungi, and an association between improved survival and lower levels of MBL in humans with pancreatic cancer (5).

MBL peptides trimerize to form a subunit and these subunits further oligomerize to form very high mol wt (HMW) multimers (2). MBL species ranging from monomers to hexamers of the MBL subunit are observed in human serum and these forms show different mannan binding ability (with negligible mannan binding by monomer, dimer, or trimer of the MBL subunit) (6). Levels of MBL are genetically determined and may alter susceptibility to specific infections in humans (2,7). Genome-wide association studies have shown that several genetic variants (8,9) in the *MBL2* gene determine the concentration of circulating MBL, with specific variants being unable to form multimers of the MBL subunit beyond a dimer (10).

MBL undergoes several post-translational modifications including hydroxylation of proline and lysine residues, glycosylation of hydroxylated lysine, and disulphide bond formation to achieve the HMW multimerized structure (11). The collagen-like domain includes several of these post-translational modifications and is essential for the interaction of MBL with mannose-associated serine protease (12) which leads to activation of the complement pathway. The importance of the collagen-like domain is further highlighted by the finding that people who carry variant alleles with three single-base substitutions (MBL-B, -C, and

[1]Cambridge Institute for Medical Research, University of Cambridge, Cambridge, United Kingdom
[2]Department of Biological Sciences, Cork Institute of Technology, Cork, Ireland
[3]School of Biochemistry and Cell Biology, University College Cork, Cork, Ireland

Correspondence: Dr. Patrick H. Maxwell, FRCP, FMedSci, School of Clinical Medicine, Cambridge Institute for Medical Research, University of Cambridge, The Keith Peters Building, Cambridge CB2 0QQ, United Kingdom. Email: regius@medschl.cam.ac.uk

-D) in the collagen-like domain have very low circulating MBL levels (2). Despite the significance of this region in controlling MBL oligomerization and function, the enzymes responsible for prolyl hydroxylation and the relevance of this modification to MBL assembly and function are not well studied.

The 2-oxoglutarate (2-OG)–dependent dioxygenases (2OGDD) are a superfamily of enzymes whose functions include hydroxylation of proteins and DNA in mammalian cells (13). Enzymes in this family are involved in various cellular processes including collagen stabilization (14), oxygen sensing (15,16), DNA repair (17,18), and carnitine biosynthesis (19). These enzymes contain iron(II) (Fe^{2+}) at the active site and catalyze the simultaneous oxidation of 2-OG and a substrate in the presence of oxygen to yield succinate and carbon dioxide (13). Two structurally related sets of enzymes which are of interest as candidates to hydroxylate proline residues in MBL are the collagen prolyl-4-hydroxylases (CP4H) and the prolyl hydroxylase domain (PHD) enzymes. These enzymes differ in their target substrates as well as affinity to different cofactors including oxygen, ascorbic acid, and 2-OG (13). CP4H hydroxylates collagen at proline residues in X-Pro-Gly motifs and inhibition of CP4H activity or mutation in the collagen domains can lead to improper folding and structural abnormalities of collagen chains, resulting in various diseases (14). PHD enzymes, on the other hand, hydroxylate specific proline residues in the α subunits of hypoxia inducible factor (HIF) (15). Under hypoxia (low oxygen), the α subunit of HIF is stabilized (16), forms a complex with the β subunit of HIF, and activates transcription of a broad range of target genes. In kidney and liver, stabilization of HIFα results in increased expression of erythropoietin (EPO) (20), a hormone involved in erythropoiesis. Stabilizing HIFα by inhibiting PHD enzymes has been validated as a therapeutic approach to increase EPO levels, and several PHD inhibitors are currently undergoing late-stage clinical trials for the treatment of anemia related to CKD (21–24).

In this study, we first sought to identify the enzyme responsible for hydroxylation of proline residues in MBL. We used pharmacologic and genetic methods to show that this hydroxylation is mediated by CP4H. We also investigated the role of prolyl hydroxylation in oligomerization and function of MBL. We finally tested the effects of PHD inhibitors in clinical development on their ability to affect MBL. We observed significant variation in the effects of PHD inhibitors, with roxadustat inhibiting hydroxylation and oligomerization of MBL, whereas molidustat did not affect oligeromization or prolyl hydroxylation of MBL. Vadadustat, on the other hand, suppressed both prolyl hydroxylation and lysyl glycosylation. Our results highlight the potential for off-target effects of PHD inhibitors on CP4H substrates including MBL. Our results also suggest that effects on MBL may provide a useful method of assaying specificity of PHD inhibitors.

Materials and Methods

Cell Culture and Reagents

HEK293S cells were obtained from ATCC (Gaithersburg, MD). Cells were cultured in DMEM (high glucose, catalog number D6429; Sigma-Aldrich) supplemented with 10% FBS (catalog number 10270106; ThermoFisher Scientific) and 1% penicillin/streptomycin (catalog number P0781; Sigma-Aldrich) (medium 1). For experimental analysis and drug treatments, the cells were washed with PBS (catalog number D8537; Sigma-Aldrich) and cultured in EX-CELL 293 serum-free medium (catalog number 14571C; Sigma-Aldrich) supplemented with 6 mM Glutamax (catalog number 35050061; ThermoFisher Scientific), 12 mg/L calcium chloride (catalog number C5670; Sigma-Aldrich), and 50 mg/L ascorbic acid (catalog number JTB1907829; J. T. Baker) (medium 2).

Dimethyloxaloylglycine (DMOG; catalog number A4506) and molidustat (catalog number BAY85-3934) were purchased from ApexBio Technology. Roxadustat was purchased from Cayman Chemical (catalog number Cay15294-50). 2,2′-Bipyridyl was purchased from Sigma-Aldrich (catalog number D216305). Stock solutions were prepared in DMSO (catalog number D8418; Sigma-Aldrich), except for DMOG which was prepared in water.

Stable Transfection of *MBL2* Gene

The complete open-reading frame of human *MBL2* (accession number NM_000242) tagged with Myc-DDK (catalog number RC210143) and the transfection reagent, Turbofectin 8.0 (catalog number TF81001), were purchased from OriGene Technologies Inc. Approximately 24 hours before transfection, approximately 10^5 cells were plated in each well of a 12-well plate to obtain 50%–70% confluency at the time of transfection. Plasmid DNA (0.5 μg) was added in 50 μl of Opti-MEM I (catalog number 31985062; ThermoFisher Scientific) and vortexed gently. Turbofectin 8.0 (1.5 μl) was added to the diluted DNA and pipetted gently, followed by a 15 minute incubation at room temperature. The mixture was added dropwise to the cells. After 48 hours, the cells were passaged and cultured with 1 mg/ml Geneticin (G418, catalog number 10131027; ThermoFisher Scientific). To select individual clones, limiting dilution was performed as follows: the G418-selected cells were plated on 96-well plates at a density of 0.5 cells per well. Wells containing single colonies were expanded as clones for further analysis.

CRISPR/Cas9 Knockdown

A pool of three plasmids each encoding Cas9 nuclease, green fluorescent protein, and guide RNA specific for either PHD2 (catalog number Sc-403334) or P4HA1 (catalog number Sc-407173) were purchased from Santa Cruz Biotechnology Inc. After 24–48 hours of transfection of the plasmids with Turbofectin 8.0 (as described above), cells positive for green fluorescent protein were isolated using a Becton Dickinson Influx cell sorter. Western blotting was performed to confirm reduction in protein expression in MBL2-expressing 293 cells.

Immunoblotting

At the time of sample collection, the supernatant from the cells was removed (either collected or aspirated) and the cells were washed once with cold (4°C) PBS and urea lysis buffer containing 8 M urea, 10% glycerol, 1% SDS, 10 mM Tris-hydrochloride (pH 6.8), and Complete Protease Inhibitor Cocktail (catalog number 11697498001;

Sigma-Aldrich) was then added directly to the cells. The lysate was collected and ultrasonication was performed at 4°C. Samples were diluted (1:10) before protein quantification using the Pierce BCA protein assay (catalog number 23227; ThermoFisher Scientific) according to the manufacturer's protocol.

Protein (50 μg) was mixed with 4× Laemmli sample buffer (catalog number 1610747; Bio-Rad) with or without β-mercaptoethanol (catalog number M6250; Sigma-Aldrich). Specific samples were denatured by boiling at 95°C for 5 minutes. The lysate was fractionated by SDS-PAGE and transferred to a polyvinylidene difluoride membrane according to the manufacturer's protocol (Bio-Rad). The membrane was rinsed with methanol and water and subsequently incubated with Ponceau S (catalog number P7170; Sigma-Aldrich) to assess protein transfer. The membrane was blocked using 5% nonfat milk in Tris-buffered saline/Tween 20 (TBST; 10 mM Tris, pH 8.0, 150 mM sodium chloride, 0.1% Tween 20) for 60 minutes on a shaker. After rinsing with TBST, the membrane was incubated for 1 hour at room temperature or overnight at 4°C with antibodies against human MBL2 (1:1250 dilution, catalog number ab26277; Abcam), HIF1α (1:500 dilution, catalog number 14179; Cell Signaling), β-actin (1:40,000 dilution, catalog number A2228-200UL; Sigma-Aldrich), α-tubulin (1:1000 dilution, catalog number 2144; Cell Signaling), P4HA1 (1:1000 dilution, catalog number NBP1-84398; Novus Biologicals), or PHD2 (1:1000 dilution, catalog number NB100-137; Novus Biologicals) on a shaker. Membranes were washed three times for 15 minutes each with TBST followed by incubation for 1 hour with IRDye 680CW goat anti-rabbit IgG secondary antibody (1:20,000 dilution, catalog number 925-68071; Li-Cor), or IRDye 800CW goat anti-mouse IgG secondary antibody (1:20,000 dilution, catalog number 925-32210; Li-Cor), or donkey anti-rabbit horseradish peroxidase secondary antibody (1:20,000 dilution, catalog number A120-208P; Bethyl Laboratories) at room temperature. Membranes were washed three times for 15 minutes each with TBST and developed with enhanced chemiluminescence (when secondary antibody was horseradish peroxidase conjugated) or imaged using the Odyssey CLx imaging system (Li-Cor).

ELISA for MBL

The supernatant was collected after 24 hours of incubation and was sterile filtered or centrifuged to remove cell debris and then stored at −80°C. MBL concentration was measured using MBL2 DuoSet ELISA (catalog number DY2307; R&D Systems) according to the manufacturer's protocol. For mannan-based ELISA, the MBL capture antibody was replaced by 10 μg/ml mannan in carbonate/bicarbonate buffer (15 mM sodium carbonate, 35 mM sodium bicarbonate, and 1.5 mM sodium azide in deionized water, final pH 9.6).

Sucrose Density Gradient

Stock solutions of 15%, 27%, 38%, and 50% sucrose were prepared and stored at 4°C. The Sw55Ti rotor and buckets were precooled at 4°C. First, using a needle and syringe, 0.4 ml of 15% sucrose solution was added to the polycarbonate centrifuge tubes (catalog number 349622; Beckman Coulter), followed by a 27% solution below the 15% layer. This process was repeated for 38% and finally for 50% sucrose solution. The layers were incubated at 4°C for 1 hour and 0.4 ml of supernatant was gently added to the top before ultracentrifugation at 55,000 rpm for 2 hours at 4°C. After ultracentrifugation, the 2 ml sample was collected as ten fractions (200 μl each) or two fractions (1000 μl each) by gently aspirating the top layer.

Immunoprecipitation

For isolation of MBL, cells were cultured in five 100-mm dishes in medium 1 until they reached 70% confluency. The medium was removed and the cells were washed with PBS and cultured in medium 2 for 24 hours with different compounds. The supernatant from five dishes was pooled and sterile filtered using Stericup Quick Release Millipore Express PLUS 0.22 μm PES (catalog number S2GPU02RE; EMD Millipore). The supernatant was concentrated using Amicon Ultra-15 centrifugal filters (catalog number UFC901024; Merck Millipore Ltd.) and used for immunoprecipitation using the μMACS DYKDDDDK Isolation Kit (catalog number 130-101-591; Miltenyi Biotec) according to the manufacturer's protocol. The isolated MBL was run on an SDS-PAGE gel and stained using InstantBlue Protein stain (catalog number ISB1L; Expedeon) and bands were excised for mass spectrometry.

Mass Spectrometry of Peptides

Samples were reduced, alkylated, and digested in gel using trypsin. The resulting peptides were analyzed by liquid chromatography with mass spectrometry using an Orbitrap Fusion Lumos coupled to an Ultimate 3000 RSLCnano UHPLC equipped with a 100-μm internal dimension × 2-cm Acclaim PepMap Precolumn (ThermoFisher Scientific) and a 75-μm internal dimension × 50-cm, 2-μm particle Acclaim PepMap RSLC analytical column. Loading solvent was 0.1% formic acid (FA) with analytical solvents A (0.1% FA) and B (80% acetonitrile plus 0.1% FA). Samples were loaded at 5 μl/min loading solvent for 5 minutes before beginning the analytical gradient. The analytical gradient was 3%–40% solvent B over 42 minutes, rising to 95% solvent B by 45 minutes, followed by a 4 minute wash at 95% solvent B, and equilibration at 3% solvent B for 10 minutes. Columns were held at 40°C. Data were acquired in a data-dependent acquisition fashion with the following settings: MS1 acquisition settings: 375–1500 m/z window, 120,000 resolution, 4×105 automatic gain control (AGC) target, 50 ms maximum injection time; MS2 acquisition settings: quadrupole isolation at an isolation width of m/z 1.6, high-energy collisional dissociation fragmentation (NCE 30) with fragment ions scanning in the Orbitrap from m/z 110, 5×104 AGC target, 100 ms maximum injection time. Dynamic exclusion was set to ±10 ppm for 60 seconds. MS2 fragmentation was triggered on precursors 5×104 counts and above.

To identify possible modifications of MBL, raw files were processed using PEAKS Studio (version X, Bioinformatics Solutions Inc.) with the following parameters: trypsin digestion; human database (UniProt reference proteome downloaded December 18, 2018 containing 21,066 proteins) with additional contaminant database (containing 246 common

contaminants); oxidation (M), carbamidomethylation (C), hydroxylation (P, K, D, N, R, Y), glucosylgalactosyl hydroxylation (K) as variable modifications at the PEAKS DB stage, 314 PEAKS built-in modifications at the PEAKS PTM stage; amino acid mutations identification enabled at the SPIDER stage.

Statistical Analysis

All data were analyzed using GraphPad Prism. Either two-way ANOVA followed by Bonferroni post-test or one-way ANOVA with Tukey's post-hoc test was used for assessing significance with $\alpha=0.05$.

Results

Recombinant MBL Oligomers Expressed in Stably Transfected HEK293 Cells Show Mannan-Binding Ability

MBL oligomers were detected in both intracellular (lysates, Figure 1A) and extracellular compartments (supernatant, Figure 1B). The secretion of monomers was negligible in the supernatant and very HMW MBL species were enriched in the supernatant as compared with lysate. As expected, human serum (from an A/A individual) also contained very HMW forms (Supplemental Figure 1).

We next separated the secreted MBL from 293 cells into ten fractions (fraction 1 [F1], lowest mol wt; F10, highest mol wt) using sucrose density gradient centrifugation (15%–50%) (Figure 1B). The abundance of total and functional forms of MBL oligomers was quantified using sandwich ELISA coated with capture antibody for MBL and mannan, respectively (Figure 1C). We evaluated the mannan-binding efficiency, defined by the percentage of MBL bound to mannan in a fraction relative to total MBL in that fraction, and observed >60% of the MBL in F7–F10 was able to bind to mannan (Figure 1D). These fractions contained very HMW forms of MBL with high mannan-binding efficiency consistent with these forms being the most functional in terms of mannan binding. F1–F3, which consisted mainly of MBL dimer and trimer, showed negligible mannan-binding ability. F5 and F6 showed intermediate binding to mannan (Figure 1, C and D, Supplemental Figure 2).

MBL Oligomerization Is Inhibited by a Pan 2-OG–Dependent Hydroxylase Inhibitor, DMOG

To investigate the role of prolyl hydroxylation on MBL oligomerization, we used DMOG, a nonselective inhibitor of the 2OGDD enzyme superfamily which includes both CP4H and PHD enzymes. DMOG treatment led to suppression of HMW oligomers of MBL (Figure 2A, Supplemental Figure 3). Treatment of cells with 2,2′-Bipirydyl (BP), an iron-chelating compound which inhibits enzymes dependent on Fe(II) including the 2OGDD superfamily, also suppressed the generation of HMW multimers. In addition, BP increased the mobility of the monomeric, dimeric, and trimeric species on the SDS-PAGE gel which was not observed with DMOG (Figure 2A), consistent with inhibition of both hydroxylation and glycosylation of MBL. Both BP and DMOG also led to stabilization of HIF1α, confirming they inhibited the PHD enzymes at the concentrations used in the study (Figure 2A).

To further analyze the distribution of MBL oligomers in the supernatant, we divided the supernatant MBL into two pools: low mol wt (LMW) MBL present in F1–F5 (light) and HMW MBL present in F6–F10 (heavy). We observed that both DMOG- and BP-treated cells showed significant reduction in secretion of MBL oligomers in F6–F10 relative to control (Figure 2B). The relative percentage of MBL in the heavy fractions (relative to total secreted MBL) was significantly decreased by both DMOG and BP (Figure 2C). The relative abundance of MBL in ten fractions highlighted an increased proportion of LMW MBL, specifically in F3 and F4 and a reduced proportion in F6–F10 (Figure 2D). Notably, we observed that very HMW forms of MBL were decreased intracellularly, indicating that reduction in formation of MBL oligomers is likely the dominant mechanism for reduced production of very HMW MBL, rather than an effect on secretion. The suppression of secretion of HMW oligomers by DMOG suggests that hydroxylation is required for formation and secretion of very HMW oligomers of MBL (more than two tetramers, *i.e.*, molecular mass of 240 kDa) and that this hydroxylation is 2-OG dependent.

P4HA1 Regulates Hydroxylation and Oligomerization of MBL

To further identify the 2OGDD enzymes that may be responsible for MBL hydroxylation, we used CRISPR/Cas9 to knockdown (KD) PHD2 (the predominant PHD isoform regulating HIF in most cell types (25)) and P4HA1 (alpha subunit of the collagen prolyl hydroxylase enzyme). The expression of other PHD enzymes (PHD1 and PHD3) was not detectable by us on Western blot of HEK293 lysates (data not shown). A pool of PHD2 KD cells showed substantial reduction in PHD2 expression and led to robust HIF1α stabilization (Figure 3A). PHD2 KD cells showed similar intracellular MBL oligomer distribution to control cells. The secretion of MBL oligomers was not significantly affected by PHD2 KD (Figure 3B). The relative proportion of MBL in HMW fractions secreted by the PHD2 KD was also similar to that of control cells (Figure 3C).

As expected, a pool of cells treated with P4HA1 single guide RNA led to a substantial reduction in P4HA1 protein expression (Figure 3A). P4HA1 KD cell lysate showed reduced HMW oligomers of MBL (Figure 3A). These cells showed an increase of LMW fractions and a suppression of HMW fractions in the secreted MBL (Figure 3D). The relative proportion of HMW MBL was also suppressed significantly (Figure 3E). The MBL abundance in ten fractions separated by sucrose gradient is shown in Figure 3, F and G. The mannan-binding efficiency of the MBL in pooled LMW and HMW fractions after P4HA1 KD was similar to control (Supplemental Figures 4 and 5), with the LMW fraction binding mannan much less efficiently. These data imply that P4HA1 is required for formation of very HMW oligomers of MBL in this system.

PHD Inhibitors Undergoing Clinical Trials Can Inhibit MBL Oligomerization

We next studied the effect of various PHD inhibitors which are undergoing clinical trials for the treatment of anemia related to renal disease. PHD enzymes and collagen

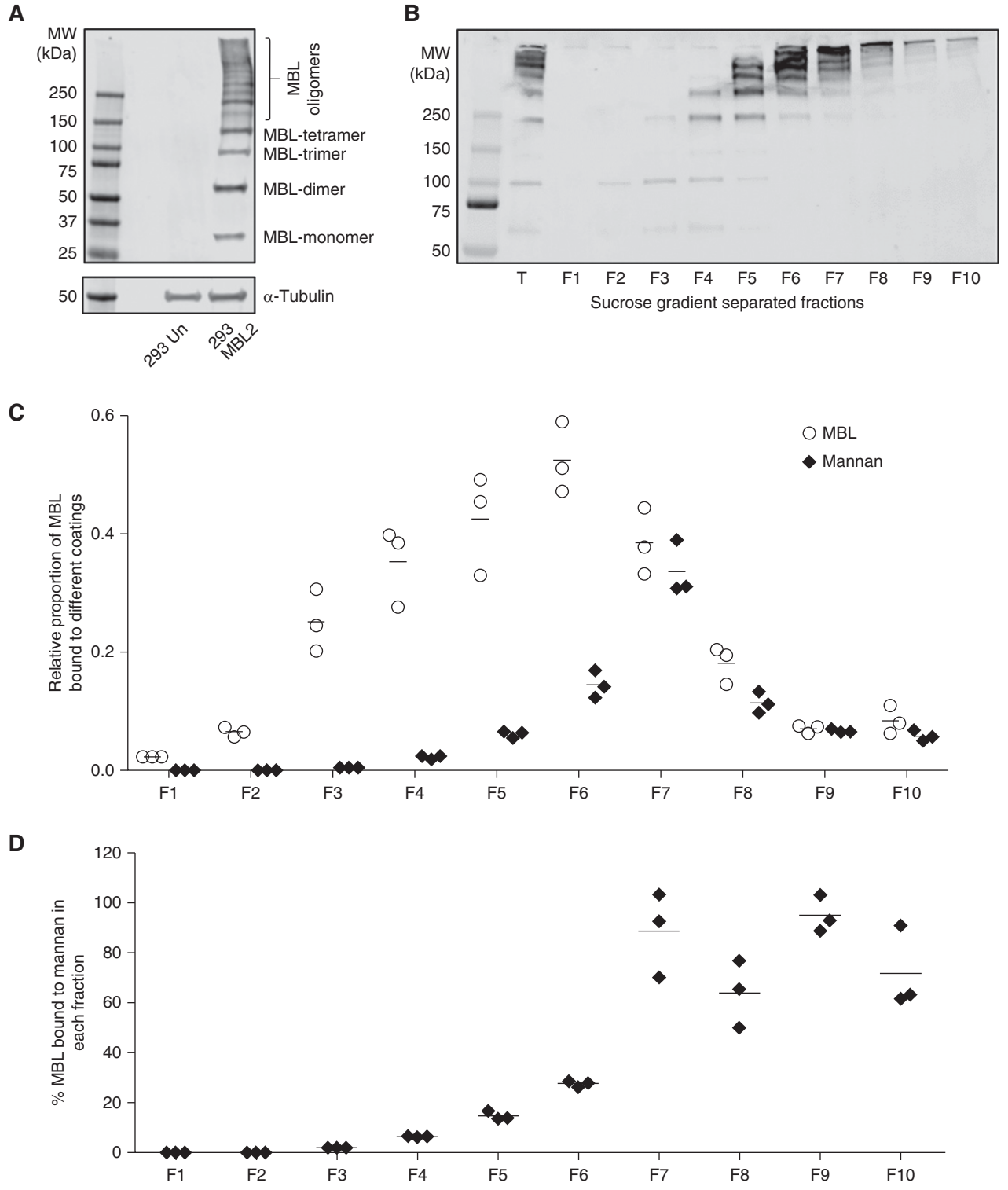

Figure 1. | Characterization of recombinant MBL mannose-binding lectin (MBL) expressed in 293 cells. (A) Representative Western blot showing the expression of MBL in protein lysates of cells transfected to express MBL. (B) The secreted form of MBL was detected by Western blot and the distribution of different forms of MBL in ten fractions separated by sucrose density gradient are shown. (C) The quantification of MBL in various fractions bound to either MBL capture antibody (open circles) or mannan (closed diamonds) coating on the ELISA plates. (D) Proportion of MBL (%) present in a fraction (detected by capture antibody) that binds to mannan-coated plates. Data from three biologic replicates are shown. Uncropped blots are provided in Supplemental Figure 2. MW, mol wt; F, fraction; F1, lowest density; F10, highest density; T, total supernatant.

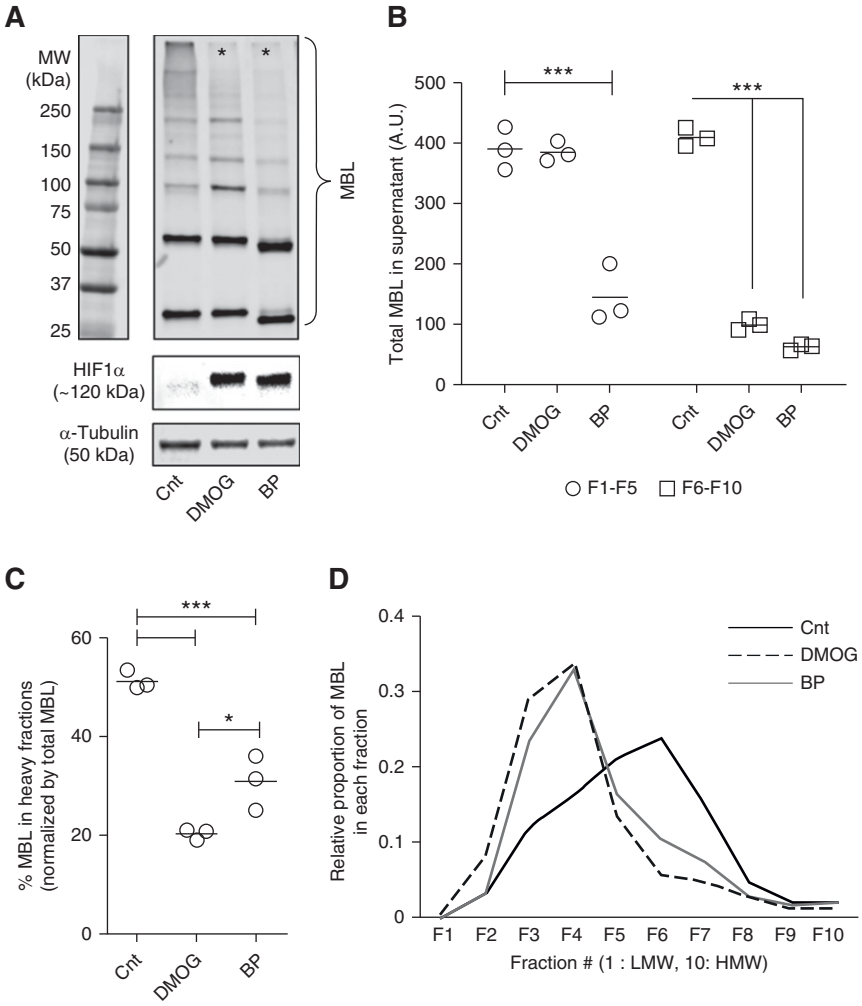

Figure 2. | MBL oligomerization is 2-oxoglutarate dependent. (A) Lysates from cells expressing MBL after treatment with dimethyloxaloylglycine (DMOG; 1 mM) or 2,2′-Bipirydyl (BP; 0.5 mM) are shown. (B) Secreted MBL in light fraction (F1–F5) or heavy fraction (F6–F10) separated by sucrose gradient after treatment with DMOG or BP is shown. Each data point represents a biologic replicate. (C) Quantification of percentage of heavy fraction (normalized by total MBL) is shown. Each data point represents a biologic replicate. *$P<0.05$, ***$P<0.001$. (D) Representative distribution of relative proportion of secreted MBL (normalized by total secreted MBL) in ten fractions separated by sucrose density gradient for one sample from each group is shown. Uncropped blots are provided in Supplemental Figure 3. HIF1α, hypoxia inducible factor 1 α; HMW, high mol wt; LMW, low mol wt; Cnt, control (cells expressing MBL and treated with DMSO).

prolyl hydroxylase enzymes are structurally closely related and use the same cosubstrates (2-OG and oxygen). Thus there is the potential that PHD inhibitors may inhibit CP4H activity in addition to their action on PHD enzymes. Indeed, in a recent study, we showed hydroxylation of complement C1q is mediated by CP4H and we found that roxadustat (a PHD inhibitor now approved for use in China and which has completed phase III clinical trials in other countries (26)) inhibited this action of CP4H. We investigated the effects of roxadustat, vadadustat, and molidustat on oligomerization and secretion of MBL. These PHD inhibitors stabilized HIF1α as expected (Figure 4A, Supplemental Figure 6). Roxadustat and vadadustat showed significant reduction in the intracellular HMW oligomers of MBL (Figure 4A). Moreover, vadadustat also resulted in a shift in mol wt of MBL, suggesting that it may also inhibit glycosylation of MBL in a similar fashion to BP. Both roxadustat and vadadustat led to a significant reduction in secretion of MBL in HMW fractions, whereas the LMW fractions were not significantly affected as compared with control (Figure 4B). In contrast, molidustat did not affect the intracellular or extracellular MBL oligomer distribution (Figure 4, A and B). The proportion of MBL in HMW fractions was significantly reduced by roxadustat and vadadustat (Figure 4, C and D). These data imply a significant difference in the specificity of these PHD inhibitors, with molidustat showing less effect on MBL.

Prolyl Hydroxylation Is Sensitive to Roxadustat and Vadadustat, but Not Molidustat

We next analyzed the post-translational modifications present in the recombinant MBL by immunoprecipitating MBL from the supernatant and using mass spectrometry (Supplemental Figure 7). The hydroxylation and glycosylation post-translational modifications that have reached the significance threshold (Ascore>20, PEAKS (27–29)) are shown

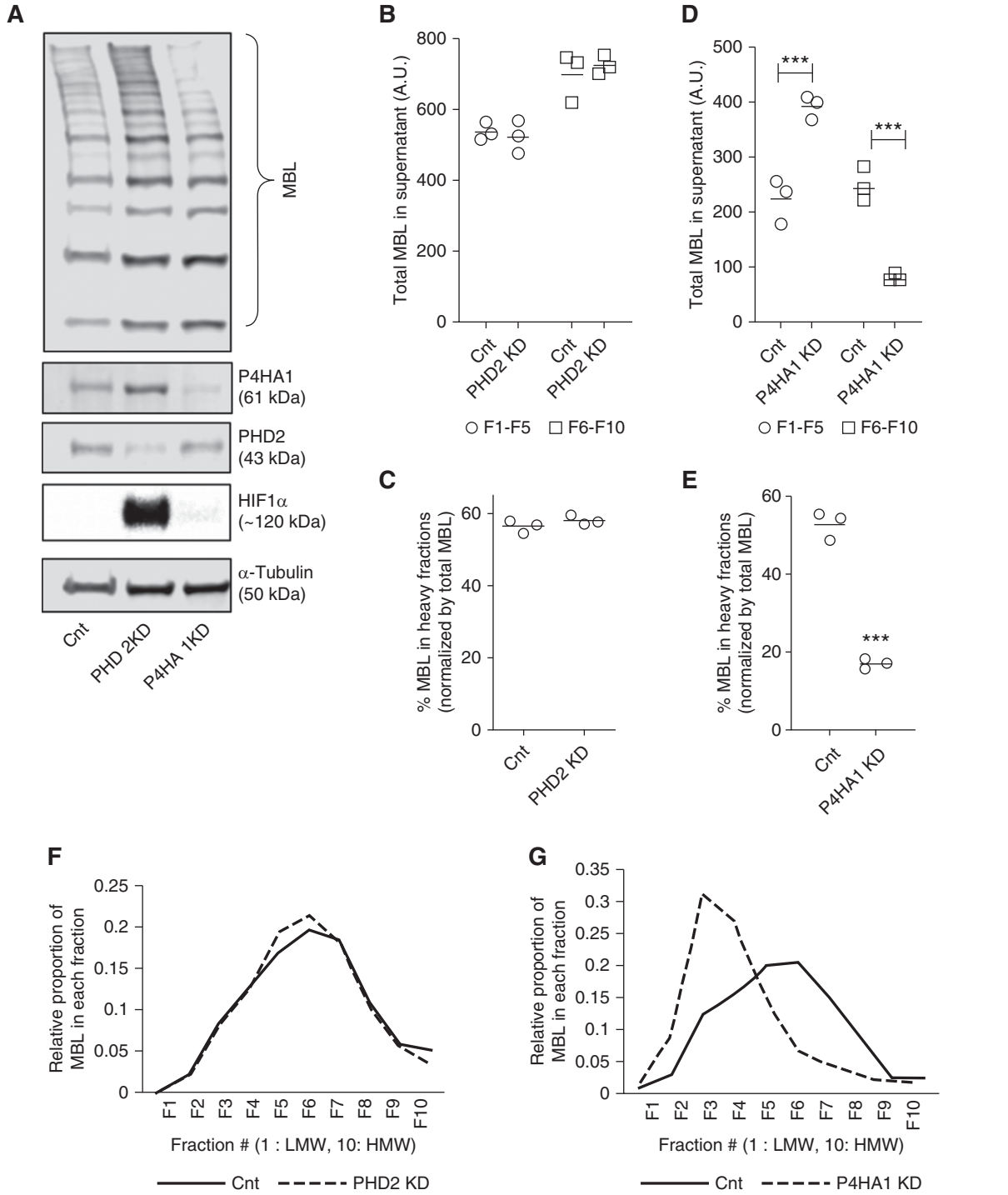

Figure 3. | **P4HA1 mediates oligomerization of MBL.** (A) Representative Western blot showing the effects of prolyl hydroxylase domain 2 (PHD2) knockdown (KD) or P4HA1 KD on expression of MBL, P4HA1, PHD2, HIF1α, and α-tubulin. Secreted MBL in light fraction (F1–F5) or heavy fraction (F6–F10) separated by sucrose gradient in (B) PHD2 KD cells and (C) P4HA1 KD cells is shown. Each data point represents a biologic replicate. Quantification of percentage of heavy fraction (normalized to total MBL) is shown for (D) PHD2 KD and (E) P4HA1 KD cells. ***$P<0.001$. Representative distribution of relative proportion of secreted MBL (normalized to total secreted MBL) in ten fractions separated by sucrose density gradient for one sample from each group is shown for (F) PHD2 KD and (G) P4HA1 KD in comparison with control. Uncropped blots are provided in Supplemental Figure 5.

above the protein sequence. We observed that all prolyl hydroxylation sites and the majority of the lysyl hydroxylation sites were within the collagen-like domain of MBL, which is consistent with the literature (11).

We next analyzed the effects of these PHD inhibitors on post-translational modifications in the collagen-like domain of MBL. The lysate and supernatant from the samples treated with respective PHD inhibitors are shown in

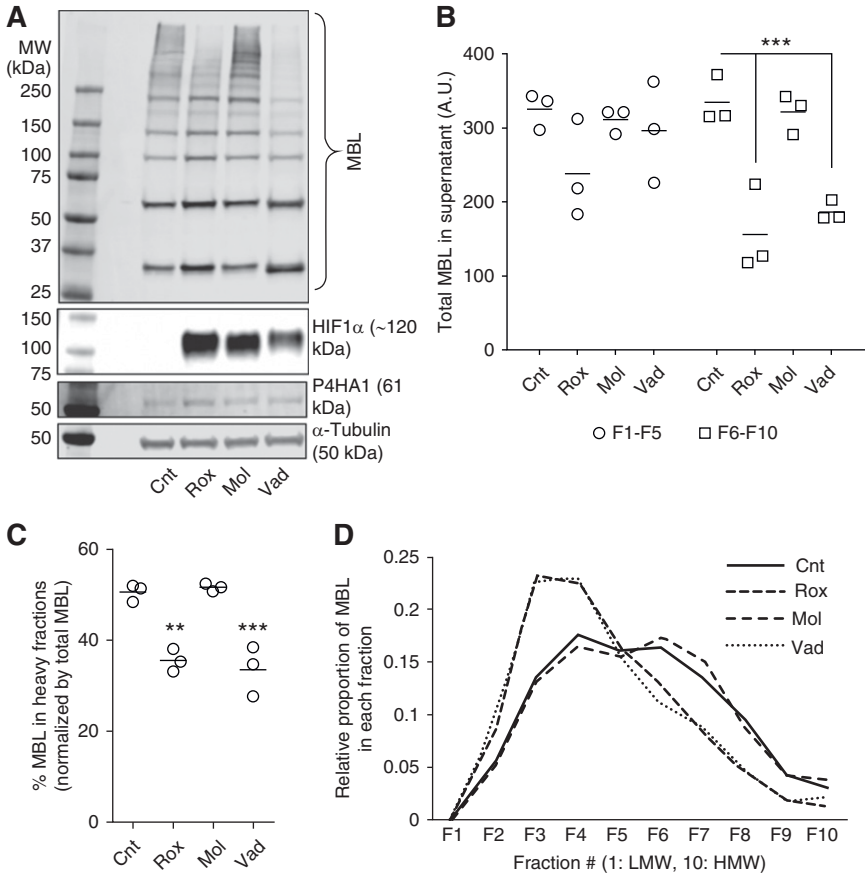

Figure 4. | Some PHD inhibitors inhibit MBL oligomerization. (A) Representative Western blot showing the effects of PHD inhibitors (roxadustat [Rox], molidustat [Mol], and vadadustat [Vad], all at 10 μM) on expression of MBL, P4HA1, HIF1α, and α-tubulin. (B) Secreted MBL in light fraction (F1–F5) or heavy fraction (F6–F10) separated by sucrose gradient after 24-hour treatment with respective PHD inhibitors. (C) Quantification of the percentage of secreted MBL in the heavy fraction (compared to total MBL) in samples treated with different PHD inhibitors is shown. $^{**}P<0.01$, $^{***}P<0.001$. (D) Representative distribution of relative proportion of secreted MBL (normalized to total secreted MBL) in ten fractions separated by sucrose density gradient for one sample from each group. Uncropped blots are provided in Supplemental Figure 6.

Figure 5, A and B (Supplemental Figure 8). Both lysate and supernatant show reduced HMW forms of MBL in roxadustat and vadadustat, consistent with our previous findings. The supernatant was further concentrated and used for mass spectrometry.

We focused on the collagen-like domain of MBL and calculated the total area under the peak of peptides in this region (both modified and unmodified). We next normalized the area of individual peptides in this collagen-like domain to the total area of peptides in this region to determine the relative abundance of various modified peptides. We observed a decrease in hydroxylated peptides in the collagen-like domain spanning the region between 40 and 99 after treatment with roxadustat and vadadustat (Figure 5C). The prolyl hydroxylated peptides accounted for 50%–60% of the collagen-region peptides in control and molidustat-treated cells. In roxadustat- and vadadustat-treated cells, on the other hand, they accounted for roughly 10% of the collagen-region peptides. We next studied the effect of these PHD inhibitors on the lysyl hydroxylation and glycosylation in the collagen region. We observed the effects of roxadustat were specific to prolyl hydroxylation because the area of lysyl hydroxylated and/or glycosylated peptides was not suppressed by roxadustat (Figure 5D). Vadadustat, on the other hand, suppressed the lysyl modifications, which is consistent with the increased mobility of MBL on SDS-PAGE described above (Figures 4A and 5, A and B). The proportion of unmodified peptides in the collagen region was also significantly higher in the vadadustat-treated cells. These data confirm that roxadustat inhibits prolyl hydroxylation whereas vadadustat inhibits both prolyl and lysyl hydroxylation of MBL in the collagen-like domain. Molidustat showed minimal effects on MBL modifications and secretion.

Discussion

Multimeric assembly is a crucial step to generate functional MBL. Using ELISA and Western blot for MBL, we confirmed the formation of very HMW oligomers of MBL both intracellularly and secreted into the culture medium. Our *in vitro* mannan-binding assay showed that lower mol wt MBL (up to trimers of the subunit) had negligible mannan-binding ability. This is in agreement with previous studies

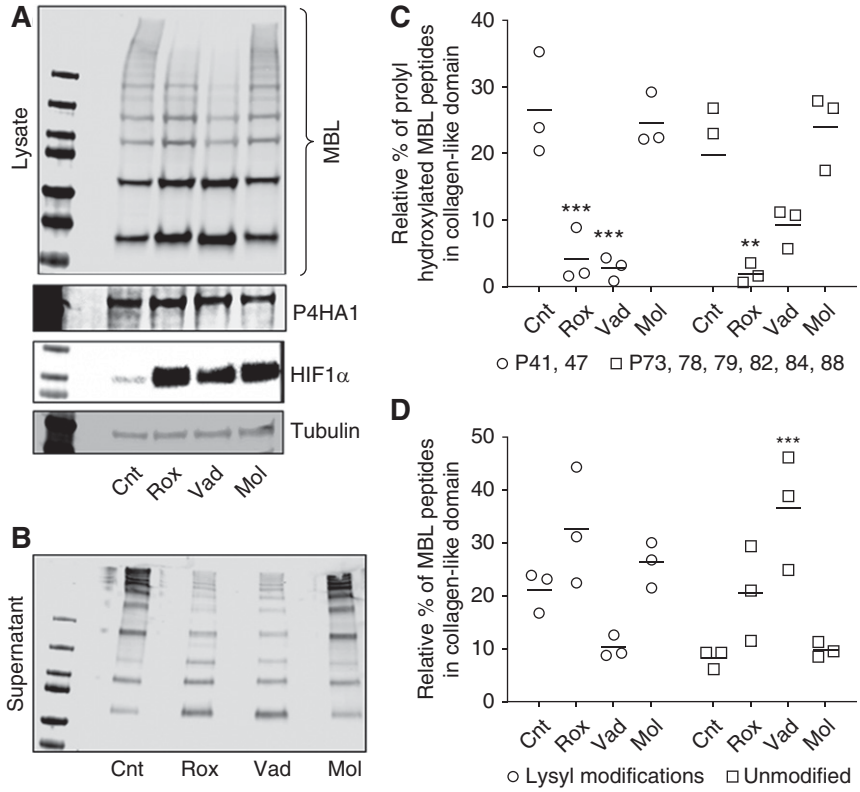

Figure 5. | **Prolyl hydroxylation in the collagen-like region is significantly inhibited by roxadustat and vadadustat but not molidustat.** Cells were treated with 10 μM of roxadustat, vadadustat, and molidustat for 24 hours. (A) Representative Western blots showing the effects of 24 hours of treatment with different PHD inhibitors on various proteins of interest in the lysates of MBL-expressing HEK293S cells. (B) Representative Western blots showing the effects of 24 hours of treatment with different PHD inhibitors on MBL secretion in the supernatant. The supernatant from three biologic replicates was concentrated and mass spectrometry analysis on the samples without knowledge of the treatments was undertaken. (C) Relative area of prolyl hydroxylated peptides covering the collagen-like domain containing hydroxylation at various proline residues (normalized to total area of MBL peptides within the collagen-like domain) in different conditions is shown. (D) Relative area of lysyl-modified (open circles) and unmodified (open squares) peptides covering the collagen-like domain (normalized by total area of MBL peptides within the collagen-like domain) in different conditions is shown. $^{**}P<0.01$, $^{***}P<0.001$. Uncropped blots are provided in the Supplemental Figure 8.

showing that functional MBL forms are at least tetramers (6,30).

We found that BP, an Fe(II) chelator, inhibited the glycosylation of MBL and multimerization. This is in agreement with previous studies where pharmacologic inhibition of glycosylation by BP was shown to inhibit the oligomerization of MBL (31). This also supports that the glycosylation of MBL is mediated by an Fe(II)-dependent enzyme; based on previous studies in rat and mouse this is likely to be lysyl hydroxylase 3 (32,33). DMOG treatment led to a selective reduction in formation and secretion of HMW forms of MBL without interfering with the glycosylation. This provides evidence that a 2OGDD enzyme is required for prolyl hydroxylation and assembly of the HMW forms of MBL.

Genetic KD of P4HA1 led to significant inhibition of HMW formation of MBL. PHD2 KD did not affect the formation of MBL oligomers, supporting that prolyl hydroxylation of the collagen-like domain of MBL as well as oligomerization of MBL is CP4H dependent and PHD independent. Finally, we used several PHD inhibitors that are currently undergoing phase III clinical trials (21,34) (roxadustat, vadadustat, and molidustat) at concentrations that stabilize HIF1α in a robust manner. Crystallography studies by Yeh *et al.* (35) showed that the mechanism of action for these drugs was *via* chelation to the active site iron. We observed that roxadustat led to inhibition of prolyl hydroxylation and formation of HMW oligomers of MBL, suggesting it inhibits CP4H activity. Importantly, we observed these effects of roxadustat at a concentration (10 μM) that is lower than the mean peak concentration in the circulation (12,200 ng/ml or 34.6 μM) in a pharmacokinetic study of healthy volunteers (36). This is in agreement with our recent study that found that roxadustat suppressed hydroxylation and secretion of complement C1q and that this was also mediated by CP4H (26). Vadadustat also led to inhibition of prolyl and lysyl hydroxylation and oligomerization of MBL, suggesting vadadustat inhibits other enzymes besides the PHDs, including CP4H. Molidustat, which has a half maximal inhibitory concentration (IC_{50}) value for PHD2 that is an order of magnitude lower than that of roxadustat and vadadustat (35), did not affect MBL oligomerization, suggesting it is more selective for PHD enzymes. Moreover, the concentration of molidustat used in our study (10 μM) is higher than the mean peak

concentration (559 ng/ml or 1.78 μM) of molidustat measured in healthy volunteers (37). This highlights the selective nature of molidustat for PHD enzymes compared with P4HA1. The fact that the distribution of mol wts of the secreted MBL was similar after both roxadustat and vadadustat is consistent with prolyl hydroxylation playing a critical role in oligomerization and secretion of HMW MBL.

Our study highlights that some of the PHD inhibitors that are in late-phase clinical trials could have off-target effects by inhibiting CP4H activity and that this would potentially include decreasing MBL activity. We envisage that our findings will stimulate those who have samples taken from appropriately consented healthy volunteers/patients treated with these PHD inhibitors to determine whether clinical use of PHD inhibitors influences circulating levels of MBL in humans. Notably, diverse other proteins such as adiponectin, collectins, ficolins, the tail structure of acetyl cholinesterase, and ectodysplasin (14) include collagen-like domains and are likely to be substrates of CP4H. These proteins may therefore also be affected by nonselective PHD inhibitors. Also, we provide evidence that another PHD inhibitor, vadadustat, can alter the activity of a further 2OGDD enzyme. It remains to be determined whether these off-target effects will be clinically significant. Importantly, partial, intermittent (three times a week) inhibition of PHD enzymes is sufficient to increase EPO and hemoglobin levels in patients with renal conditions (23,24). With these dosing strategies, potential consequences of off-target effects of PHD inhibitors (and risks associated with sustained HIF stabilization) may be minimized (38). Nevertheless, a high degree of target specificity is generally desirable in drug-development programs. Our work provides a potential approach to assess off-target effects of PHD inhibitors on CP4H using MBL as a model substrate. Because the effects on oligomerization are indicative of function of CP4H whereas the mol wt of the protein is a function of lysyl hydroxylase enzymes, effects of drugs on different enzymatic processes can be assessed.

Acknowledgments

We are grateful for the support and assistance of Dr. Robin Antrobus at the proteomics core facility. We also thank Dr. Natalie Burrows, Dr. James McCaffery, and Dr. Ana Penalver for helpful discussions.

Author Contributions

V. Bhute was responsible for data curation and formal analysis; V. Bhute and P. Maxwell conceptualized the study, wrote the original draft, reviewed and edited the manuscript, and were responsible for resources and visualization; V. Bhute, J. Harte, and J. Houghton were responsible for investigation; V. Bhute and J. Houghton were responsible for software; P. Maxwell was responsible for funding acquisition, project administration, and supervision; and all authors were responsible for methodology.

Disclosures

P. Maxwell is a scientific founder and holds equity in ReOx Ltd. He has received a speaker honorarium from Fibrogen. He is head of the School of Clinical Medicine at the University of Cambridge, which has strategic partnerships with AstraZeneca and GlaxoSmithKline, both of which are developing PHD inhibitors for the treatment of renal anemia. All remaining authors have nothing to disclose.

Funding

This work was supported by a Wellcome Trust Senior Investigator Award to P. Maxwell (096956/Z supporting V. Bhute), the National Institute for Health Research Cambridge Biomedical Research Centre, and the Rosetrees Trust. J. Harte was supported by the Cambridge Amgen Scholars Program.

Supplemental Material

This article contains supplemental material online at http://kidney360.asnjournals.org/lookup/suppl/doi:10.34067/KID.0000092020/-/DCSupplemental.

Supplemental Figure 1. Representative western blot showing the distribution of MBL in human serum.

Supplemental Figure 2. Uncropped Western blots used in Figure 1.

Supplemental Figure 3. Uncropped Western blots used in Figure 2.

Supplemental Figure 4. Uncropped Western blots used in Figure 3.

Supplemental Figure 5. Proportion of secreted MBL which binds to mannan (%) in Untransfected control and P4HA1 KD MBL expressing cells.

Supplemental Figure 6. Uncropped Western blots used in Figure 4.

Supplemental Figure 7. Mass spectrometry analysis of secreted recombinant MBL.

Supplemental Figure 8. Uncropped Western blots used in Figure 5.

References

1. Neth O, Jack DL, Dodds AW, Holzel H, Klein NJ, Turner MW: Mannose-binding lectin binds to a range of clinically relevant microorganisms and promotes complement deposition. *Infect Immun* 68: 688–693, 2000
2. Garred P, Larsen F, Seyfarth J, Fujita R, Madsen HO: Mannose-binding lectin and its genetic variants. *Genes Immun* 7: 85–94, 2006
3. Stuart LM, Takahashi K, Shi L, Savill J, Ezekowitz RAB: Mannose-binding lectin-deficient mice display defective apoptotic cell clearance but no autoimmune phenotype. *J Immunol* 174: 3220–3226, 2005
4. Walsh MC, Bourcier T, Takahashi K, Shi L, Busche MN, Rother RP, Solomon SD, Ezekowitz RAB, Stahl GL: Mannose-binding lectin is a regulator of inflammation that accompanies myocardial ischemia and reperfusion injury. *J Immunol* 175: 541–546, 2005
5. Aykut B, Pushalkar S, Chen R, Li Q, Abengozar R, Kim JI, Shadaloey SA, Wu D, Preiss P, Verma N, Guo Y, Saxena A, Vardhan M, Diskin B, Wang W, Leinwand J, Kurz E, Kochen Rossi JA, Hundeyin M, Zambrinis C, Li X, Saxena D, Miller G: The fungal mycobiome promotes pancreatic oncogenesis via activation of MBL. *Nature* 574: 264–267, 2019
6. Kjaer TR, Jensen L, Hansen A, Dani R, Jensenius JC, Dobó J, Gál P, Thiel S: Oligomerization of mannan-binding lectin Dictates binding properties and complement activation. *Scand J Immunol* 84: 12–19, 2016
7. Keizer MP, Wouters D, Schlapbach LJ, Kuijpers TW: Restoration of MBL-deficiency: Redefining the safety, efficacy and viability of MBL-substitution therapy. *Mol Immunol* 61: 174–184, 2014
8. Suhre K, Arnold M, Bhagwat AM, Cotton RJ, Engelke R, Raffler J, Sarwath H, Thareja G, Wahl A, DeLisle RK, Gold L, Pezer M, Lauc G, El-Din Selim MA, Mook-Kanamori DO, Al-Dous EK, Mohamoud YA, Malek J, Strauch K, Grallert H, Peters A, Kastenmüller G, Gieger C, Graumann J: Connecting genetic risk to disease end points through the human blood plasma proteome. *Nat Commun* 8: 14357, 2017
9. Sun BB, Maranville JC, Peters JE, Stacey D, Staley JR, Blackshaw J, Burgess S, Jiang T, Paige E, Surendran P, Oliver-Williams C, Kamat MA, Prins BP, Wilcox SK, Zimmerman ES, Chi A, Bansal N, Spain SL, Wood AM, Morrell NW, Bradley JR, Janjic N, Roberts DJ, Ouwehand WH, Todd JA, Soranzo N, Suhre K, Paul DS, Fox CS, Plenge RM, Danesh J, Runz H, Butterworth AS:

Genomic atlas of the human plasma proteome. *Nature* 558: 73–79, 2018
10. Larsen F, Madsen HO, Sim RB, Koch C, Garred P: Disease-associated mutations in human mannose-binding lectin compromise oligomerization and activity of the final protein. *J Biol Chem* 279: 21302–21311, 2004
11. Jensen PH, Laursen I, Matthiesen F, Højrup P: Posttranslational modifications in human plasma MBL and human recombinant MBL. *Biochim Biophys Acta* 1774: 335–344, 2007
12. Teillet F, Lacroix M, Thiel S, Weilguny D, Agger T, Arlaud GJ, Thielens NM: Identification of the site of human mannan-binding lectin involved in the interaction with its partner serine proteases: The essential role of Lys55. *J Immunol* 178: 5710–5716, 2007
13. Loenarz C, Schofield CJ: Expanding chemical biology of 2-oxoglutarate oxygenases. *Nat Chem Biol* 4: 152–156, 2008
14. Myllyharju J, Kivirikko KI: Collagens, modifying enzymes and their mutations in humans, flies and worms. *Trends Genet* 20: 33–43, 2004
15. Schofield CJ, Ratcliffe PJ: Oxygen sensing by HIF hydroxylases. *Nat Rev Mol Cell Biol* 5: 343–354, 2004
16. Maxwell PH, Wiesener MS, Chang GW, Clifford SC, Vaux EC, Cockman ME, Wykoff CC, Pugh CW, Maher ER, Ratcliffe PJ: The tumour suppressor protein VHL targets hypoxia-inducible factors for oxygen-dependent proteolysis. *Nature* 399: 271–275, 1999
17. Falnes P, Johansen RF, Seeberg E: AlkB-mediated oxidative demethylation reverses DNA damage in Escherichia coli. *Nature* 419: 178–182, 2002
18. Trewick SC, Henshaw TF, Hausinger RP, Lindahl T, Sedgwick B: Oxidative demethylation by Escherichia coli AlkB directly reverts DNA base damage. *Nature* 419: 174–178, 2002
19. Vaz FM, Wanders RJA: Carnitine biosynthesis in mammals. *Biochem J* 361: 417–429, 2002
20. Haase VH: Regulation of erythropoiesis by hypoxia-inducible factors. *Blood Rev* 27: 41–53, 2013
21. Maxwell PH, EckardtK-U: HIF prolyl hydroxylase inhibitors for the treatment of renal anaemia and beyond. *Nat Rev Nephrol* 12: 157–168, 2016
22. Joharapurkar AA, Pandya VB, Patel VJ, Desai RC, Jain MR: Prolyl hydroxylase inhibitors: A breakthrough in the therapy of anemia associated with chronic diseases. *J Med Chem* 61: 6964–6982, 2018
23. Chen N, Hao C, LiuB-C, Lin H, Wang C, Xing C, Liang X, Jiang G, Liu Z, Li X, Zuo L, Luo L, Wang J, Zhao MH, Liu Z, CaiG-Y, Hao L, Leong R, Wang C, Liu C, Neff T, Szczech L, Yu KP: Roxadustat treatment for anemia in patients undergoing long-term dialysis. *N Engl J Med* 381: 1011–1022, 2019
24. Chen N, Hao C, Peng X, Lin H, Yin A, Hao L, Tao Y, Liang X, Liu Z, Xing C, Chen J, Luo L, Zuo L, Liao Y, LiuB-C, Leong R, Wang C, Liu C, Neff T, Szczech L, Yu KP: Roxadustat for anemia in patients with kidney disease not receiving dialysis. *N Engl J Med* 381: 1001–1010, 2019
25. Berra E, Richard DE, Gothié E, Pouysségur J: HIF-1-dependent transcriptional activity is required for oxygen-mediated HIF-1α degradation. *FEBS Lett* 491: 85–90, 2001
26. Kiriakidis S, Hoer SS, Burrows N, Biddlecome G, Khan MN, Thinnes CC, Schofield CJ, Rogers N, Botto M, Paleolog E, Maxwell PH: Complement C1q is hydroxylated by collagen prolyl 4 hydroxylase and is sensitive to off-target inhibition by prolyl hydroxylase domain inhibitors that stabilize hypoxia-inducible factor. *Kidney Int* 92: 900–908, 2017
27. Ma B, Zhang K, Hendrie C, Liang C, Li M, Doherty-Kirby A, Lajoie G: PEAKS: Powerful software for peptide de novo sequencing by tandem mass spectrometry. *Rapid Commun Mass Spectrom* 17: 2337–2342, 2003
28. Tran NH, Zhang X, Xin L, Shan B, Li M: De novo peptide sequencing by deep learning. *Proc Natl Acad Sci U S A* 114: 8247–8252, 2017
29. Tran NH, Qiao R, Xin L, Chen X, Liu C, Zhang X, Shan B, Ghodsi A, Li M: Deep learning enables de novo peptide sequencing from data-independent-acquisition mass spectrometry. *Nat Methods* 16: 63–66, 2019
30. Teillet F, Dublet B, AndrieuJ-P, Gaboriaud C, Arlaud GJ, Thielens NM: The two major oligomeric forms of human mannan-binding lectin: chemical characterization, carbohydrate-binding properties, and interaction with MBL-associated serine proteases. *J Immunol* 174: 2870–2877, 2005
31. Ma Y, Shida H, Kawasaki T: Functional expression of human mannan-binding proteins (MBPs) in human hepatoma cell lines infected by recombinant vaccinia virus: post-translational modification, molecular assembly, and differentiation of serum and liver MBP. *J Biochem* 122: 810–818, 1997
32. Heise CT, Nicholls JR, Leamy CE, Wallis R: Impaired secretion of rat mannose-binding protein resulting from mutations in the collagen-like domain. *J Immunol* 165: 1403–1409, 2000
33. Risteli M, Ruotsalainen H, Bergmann U, Venkatraman Girija U, Wallis R, Myllylä R: Lysyl hydroxylase 3 modifies lysine residues to facilitate oligomerization of mannan-binding lectin. *PLoS One* 9: e113498, 2014
34. Akizawa T, Taguchi M, Matsuda Y, Iekushi K, Yamada T, Yamamoto H: Molidustat for the treatment of renal anaemia in patients with dialysis-dependent chronic kidney disease: design and rationale of three phase III studies. *BMJ Open* 9: e026602, 2019
35. YehT-LL, Leissing TMM, Abboud MI, Thinnes CC, Atasoylu O, Holt-Martyn JP, Zhang D, Tumber A, Lippl K, Lohans CT, Leung IKH, Morcrette H, Clifton IJ, Claridge TDW, Kawamura A, Flashman E, Lu X, Ratcliffe PJ, Chowdhury R, Pugh CW, Schofield CJ: Molecular and cellular mechanisms of HIF prolyl hydroxylase inhibitors in clinical trials. *Chem Sci (Camb)* 8: 7651–7668, 2017
36. Groenendaal-van de Meent D, den Adel M, Rijnders S, Krebs-Brown A, Kerbusch V, Golor G, Schaddelee M: The hypoxia-inducible factor prolyl-hydroxylase inhibitor roxadustat (FG-4592) and warfarin in healthy volunteers: a pharmacokinetic and pharmacodynamic drug-drug interaction study. *Clin Ther* 38: 918–928, 2016
37. Böttcher M, Lentini S, Arens ER, Kaiser A, van der Mey D, Thuss U, Kubitza D, Wensing G: First-in-man-proof of concept study with molidustat: A novel selective oral HIF-prolyl hydroxylase inhibitor for the treatment of renal anaemia. *Br J Clin Pharmacol* 84: 1557–1565, 2018
38. Maxwell PH: A new approach to treating renal anaemia. *Nat Rev Nephrol* 15: 731–732, 2019

Received: January 9, 2020 **Accepted:** March 31, 2020